

## Microstructure and Mechanical Properties of Nano-ZrO<sub>2</sub> and Nano-SiO<sub>2</sub> Particulate Reinforced AZ31-Mg Based Composites Fabricated by Friction Stir Processing

C. I. Chang<sup>a</sup>, Y. N. Wang<sup>a,b</sup>, H. R. Pei<sup>a</sup>, C. J. Lee<sup>a</sup>, X. H. Du<sup>a</sup>,  
J. C. Huang<sup>a\*</sup>

<sup>a</sup> Institute of Materials Science and Engineering; Center for Nanoscience and Nanotechnology,  
National Sun Yat-Sen University, Kaohsiung, Taiwan 804, R. O. China

<sup>b</sup> Institute of Materials Science and Engineering, Dalian University of Technology, Dalian 116024,  
P. R. China

\* Corresponding author: [jacobc@mail.nsysu.edu.tw](mailto:jacobc@mail.nsysu.edu.tw)

**Keywords:** Friction stir processing; Magnesium alloy; Nano-sized particles; Composite.

**Abstract.** Friction stir processing (FSP) has been applied to fabricate 10~20 vol% nano-sized ZrO<sub>2</sub> and 5~10 vol% nano-sized SiO<sub>2</sub> particles into an Mg-AZ31 alloy to form bulk composites under the FSP parameters of advancing speed of 800 rpm and pin rotation of 45 min/min. The microstructures and mechanical properties of the resulting composites were investigated. The clustering size of nano-ZrO<sub>2</sub> and nano-SiO<sub>2</sub> particles, measuring average ~200 nm was relatively uniformly dispersed, and the average grain size of the both Mg alloy of the composites varied within 1.0~2.0 µm after four FSP passes. No evident interfacial product between ZrO<sub>2</sub> particles and Mg matrix was found during the FSP mixing in AZ31-Mg/ZrO<sub>2</sub>. However, significant chemical reactions at the AZ31-Mg/SiO<sub>2</sub> interface occurred to form the Mg<sub>2</sub>Si phase. The mechanical responses of the nano-composites in terms of hardness and tensile properties are examined and compared.

### Introduction

The development of metal matrix composites (MMCs) has been activated by the increasing need for structural materials with high special strength and stiffness. Mg alloys with ~35% lower density compared with Al alloys have exhibited the promise as structural materials in engineering applications which require the higher special mechanical properties. Especially, the aerospace and automobile industries are actively seeking magnesium-based alloys. One of the major limitations of Mg and its alloys is their relatively low elastic modulus. However, this limitation can be circumvented by the use of harder and stiffer ceramic particulates reinforcements. An improvement such as in tribological characteristics, dimensional stability, damping capacity, and elevated temperature creep properties, can be realized by the judicious selection in type, size and volume fraction of reinforcements besides that of elastic modulus. Therefore, several methods to fabricate particulate reinforcement Mg-based composites, including molten metal infiltration [1], powder metallurgy [2], squeeze casting [3], stir casting [4] and spray forming [5], have been developed.

Friction-stir welding (FSW) is a solid-state joining processing initially developed by The Welding Institute (TWI) in United Kingdom [6]. Recently, its modification into friction stir processing (FSP) is also applied to modify the microstructure by localized grain size refinements and homogenization of precipitate particles in aluminum and magnesium alloys [7-11]. In addition, Mishra et al. [12] have mixed second phases into the matrix during FSP to fabricate surface composite. Lee et al. [13] have inserted nano-SiO<sub>2</sub> powders into the AZ61 magnesium alloy during FSP to successfully fabricate the bulk nano-SiO<sub>2</sub>/AZ61 composite. It means that FSP appears to offer another feasible route to incorporate ceramic particles into the matrix to form bulk composites.

Dispersion of nano-scaled reinforcements with a uniform manner in MMCs is a critical and difficult task owing to the high surface energy of nano-particles. The current paper presents a simple means of employing FSP to fabricate bulk Mg/nano-ZrO<sub>2</sub>/and Mg/nano-SiO<sub>2</sub> composites, and the

comparison of microstructure and mechanical properties of the composites was carried out.

## Experimental

The AZ31 billets possessed nearly equiaxed grains around 70  $\mu\text{m}$  was used in this study. The chemical composition (in mass percent) is Mg-3.02%Al-1.01%Zn-0.30%Mn. The samples subjected to FSP were cut from billet as rectangular, measuring 60 mm in width, 130 mm in length and 10 mm in thickness. The crystalline  $\text{ZrO}_2$  powder (with a monocline structure) and amorphous  $\text{SiO}_2$  powder used in this study are nearly equiaxed in shape, with an average diameter  $\langle d \rangle \sim 20$  nm and purity  $\sim 99.9\%$  and a density of 5.7  $\text{Mg/m}^3$  and 2.65  $\text{Mg/m}^3$ , respectively.

The simplified FSP machine is a modified form of a horizontal-type miller, with a 5 HP spindle. The fixed pin tool of 6 mm in diameter and 6 mm in length, and the shoulder diameter of 18 mm, and  $2^\circ$  tilt angle of the fixed pin tool were used. The FSP parameters of advancing speed of 800 rpm and pin rotation of 45 min/min were applied in the present experiment. To insert the nano-particles, one or two grooves each  $\sim 6$  mm in depth and 1.25 mm in width are cut, in which the nano-particles are filled to the desired amount before FSP. The details of the FSP procedure are referred as in our previous paper [13]. The volume fraction of  $\text{ZrO}_2$  particles and  $\text{SiO}_2$  inserted into AZ31 alloy are calculated to be around 10~20% and 5~10% for one and two grooves (denoted as 1G and 2G), respectively. More  $\text{ZrO}_2$  nano powders can be inserted into the grooves due to the heavier weight, resulting 10 vol% for the 1G and 20 vol% for the 2G samples, compared with 5 and 10 vol% for the  $\text{SiO}_2$  counterparts. The advancing direction of one to four passes (denoted as 1P to 4P) is opposite to the FSP direction for the previous pass (i.e. forward and then backward).

Vickers hardness tests were conducted using a 200 gf load for 10 s. The grain structure and the particle distribution of etched and unetched samples are examined by optical microscopy (OM) and scanning or transmission electron microscopy (SEM or TEM) with energy dispersive spectrometer (EDS). The size of clustering nano-particles is analyzed by optimas image analysis software in SEM photographs at different magnifications.

## Results and Discussions

**Microstructures.** Microstructure characterization in this study was mainly focused on the distribution and clustering of nano- $\text{ZrO}_2$  particles and the grain structures of matrix induced by dynamic recrystallization in the nugget zone. Because frictional heating and severe plastic deformation by the rotating tool are simultaneously introduced into material during FSP, therefore, it is expected that both frictional heating and plastic strain lead to the formation of dynamically recrystallized grains and the dispersing of the inserted nano- $\text{ZrO}_2$  and nano- $\text{SiO}_2$  particles in stir zones of the present Mg-based composites.

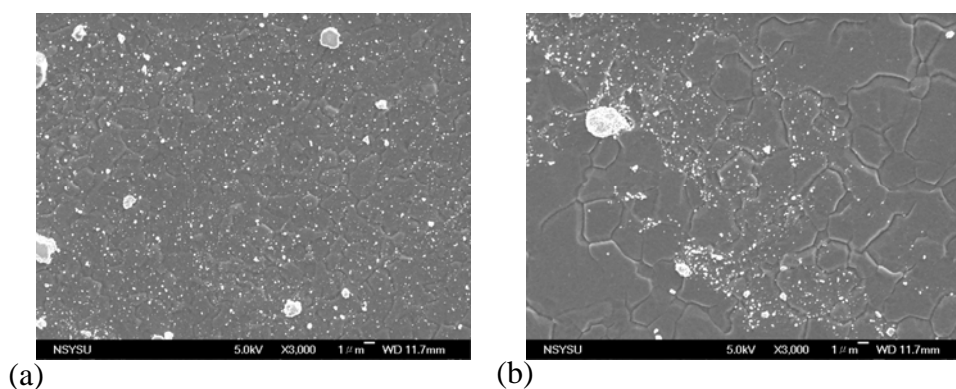


Fig. 1 SEM/SEI micrographs showing the (a) relatively homogeneous dispersion, and (b) local inhomogenization of nano-particle clusters ( $\sim 10\%$   $\text{ZrO}_2$ ) within the FSZ after one-pass FSP.

After one-pass (1P) FSP, the dispersion of the nano-particles within the central cross-sectional area of the FSZ is basically uniform, as shown in Fig. 1(a). The observed clustering particle size is frequently 0.1-2  $\mu\text{m}$ , much larger than the individual nano-particle size ( $\sim 20$  nm). In addition, some local inhomogenized areas of the particles can be found in 1P FSP sample, as shown in Fig. 1(b). The clustering size of the particles after two to four passes (2P to 4P) appears to have further reduced, as shown in Fig. 2. Meanwhile, with increasing FSP passes, the average grain size of AZ31 alloy matrix is also significantly reduced from around 70  $\mu\text{m}$  in the initial billet to 2~4  $\mu\text{m}$  in the 4P FSP samples. The summary of the clustering size of the particles and the average grain size of AZ31 alloy matrix in the 4P FSP samples are listed in Table 1.

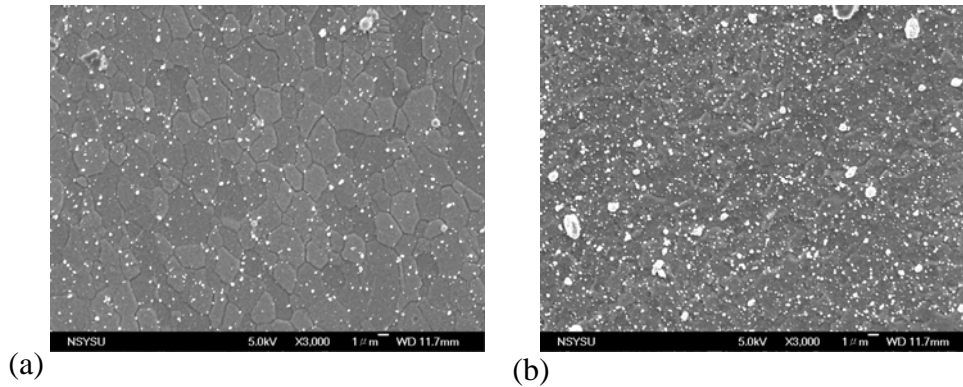


Fig. 2 SEM/SEI micrographs showing the nano-particle dispersion in (a)  $\sim 5$  vol%  $\text{SiO}_2$  particles, and (b)  $\sim 20$  vol%  $\text{ZrO}_2$  particles in 4P FSP samples.

Table 1 Summary of the average cluster size of nano-particles and the average grain size of AZ31 matrix in the 4 passes FSP composites, as well as the comparison of the mechanical properties of AZ31 alloy and AZ31-based composites.

Materials	Average grain size, $\mu\text{m}$	Particle cluster size, nm	YS, MPa	UTS, MPa	El, %
AZ31 billet	70		100	160	$\sim 9$
AZ31 after 4P FSP	$\sim 6$		120	204	$\sim 18$
$\sim 10$ vol% $\text{ZrO}_2$ (4P)	$\sim 3$	$\sim 200$	143	232	$\sim 6$
$\sim 20$ vol% $\text{ZrO}_2$ (4P)	$\sim 2$	$\sim 180$	167	255	$\sim 6$
$\sim 5$ vol% $\text{SiO}_2$ (4P)	$\sim 4$	$\sim 300$	-	-	$\sim 6$
$\sim 10$ vol% $\text{SiO}_2$ (4P)	$\sim 3$	$\sim 260$	128	258	$\sim 6$

YS: yield strength; UTS: ultimate tensile strength; El: elongation.

**XRD Results.** The XRD patterns for the transverses cross-sectional plane of the FSP composites are presented in Fig. 3. It can be seen from Fig. 3(a) that there were not other phases except a small amount of reinforcement of  $\text{ZrO}_2$  (weak peaks) and the Mg matrix in the Mg-AZ31/ $\text{ZrO}_2$  composite after 4 passes. This indicated that the crystalline  $\text{ZrO}_2$  phase is very stable, no reaction between the  $\text{ZrO}_2$  phase and Mg matrix occurred during the FSP mixing  $\text{ZrO}_2$  into the Mg-AZ31 matrix. However, some additional weak peaks identified as the  $\text{Mg}_2\text{Si}$  and  $\text{MgO}$  phases can be found in the FSP Mg-AZ31/ $\text{SiO}_2$  composite, as shown in Fig. 3(b). It is suggested that the chemical reaction between the  $\text{SiO}_2$  phase and Mg matrix would occur during the FSP mixing  $\text{SiO}_2$  into Mg-AZ31

matrix. The reaction in Mg - SiO<sub>2</sub> system can be described by the following reaction of  $4\text{Mg} + \text{SiO}_2 \rightarrow 2\text{MgO} + \text{Mg}_2\text{Si}$ . Our previous study [13] also confirmed the presence of the Mg<sub>2</sub>Si and MgO phases in the Mg-AZ61/nano-SiO<sub>2</sub> composite fabricated by the same FSP route.

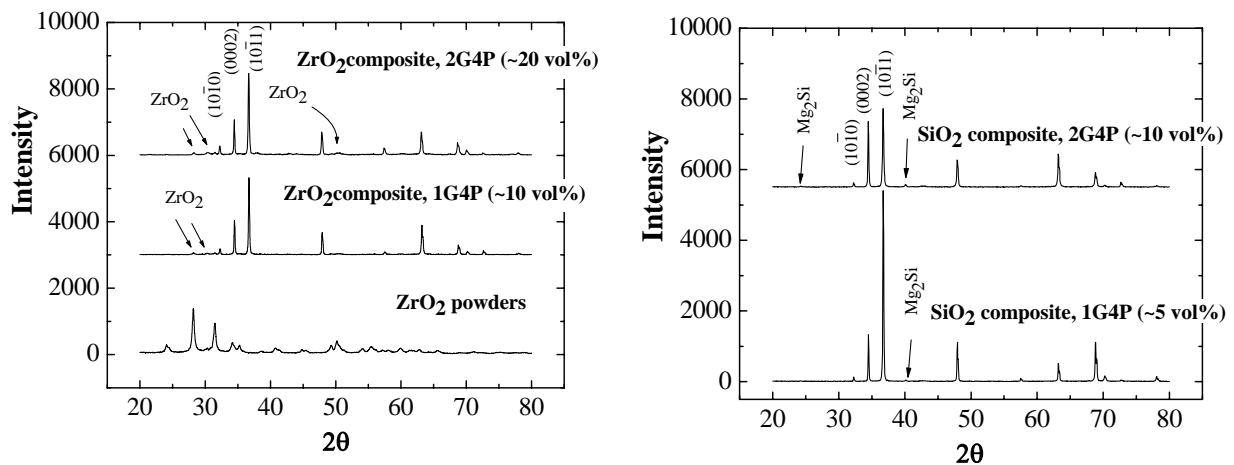


Fig. 3 X-ray diffraction for the (a) AZ31/ZrO<sub>2</sub> composites and (b) AZ31/SiO<sub>2</sub> composites prepared by 4P FSP.

**Hardness Measurement.** The typical Vickers hardness readings,  $H_v$ , measured along the central cross-section zones of the FSP samples are depicted in Fig. 4. Compared with the AZ31 alloy without ZrO<sub>2</sub> or SiO<sub>2</sub> powders reinforcements, almost a double increment of the hardness of the present composites was achieved, especially for the 2G4P sample with ~20 vol% ZrO<sub>2</sub> particle. After FSP, the scattering of microhardness within the FSP nugget zone is considered to be relatively minor, implying that the pin stirring efficiently dispersed the nano-ZrO<sub>2</sub> particles in a reasonably uniform manner, especially after more than one pass. For the AZ31 alloy without ZrO<sub>2</sub> reinforcements, after four passes FSP, the microhardness could also increase from ~50 up to ~70 due to the grain refinement from ~70  $\mu\text{m}$  down to ~6  $\mu\text{m}$  via dynamic recrystallization.

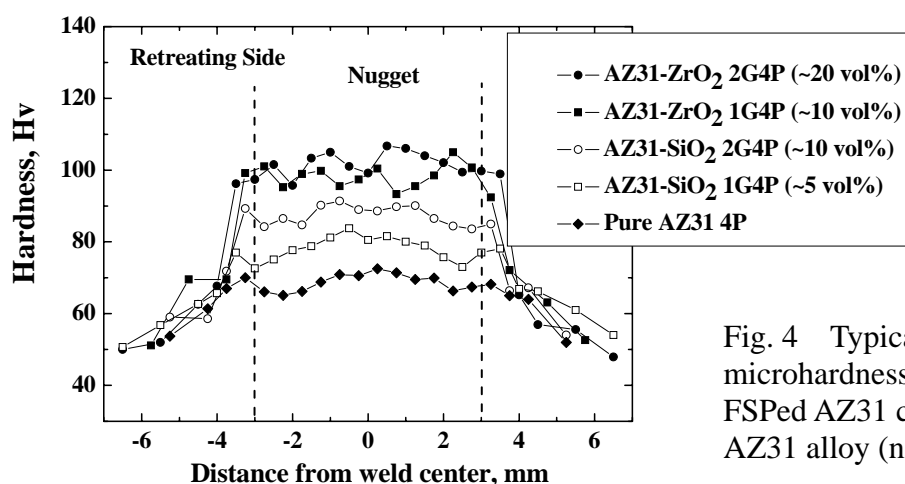


Fig. 4 Typical variation of the microhardness ( $H_v$ ) distribution in FSPed AZ31 composites and FSPed AZ31 alloy (no particles).

**Mechanical Properties.** All tensile samples were machined perpendicular to the processing direction from the central region of the weld for the room temperature tensile test. Table 1 also lists the tensile properties of AZ31 FSP alloy and composites, taking the average from two or three samples. The increases of yield stress (YS) and ultimate tensile stress (UTS) as well as tensile elongation for the FSP AZ31 alloy were mainly contributed by the grain refinement from ~70  $\mu\text{m}$  in

AZ31 billet to  $\sim 6\ \mu\text{m}$  in FSP AZ31 sample. For the FSP composite, the *YS* and *UTS* were obviously improved due to the nano-ZrO<sub>2</sub> and nano-SiO<sub>2</sub> reinforcements. Note that the *YS* and *UTS* values of the FSP AZ31 alloy specimens are all lower than those observed in the extruded or rolled AZ31 alloys possessing similar fine grain sizes of 2-6  $\mu\text{m}$  [14-15]. This is mainly a result of the special texture effect addressed elsewhere [16].

## Conclusion

- (1) Friction stir processing was successfully used to fabricate bulk Mg-AZ31 based composites with 10 ~ 20 vol% of nano-ZrO<sub>2</sub> particles and 5 ~ 10 vol% of nano-SiO<sub>2</sub> particles. The distribution of nano particles measuring  $\sim 20\ \text{nm}$  after four FSP passes resulted in satisfactorily uniform distribution.
- (2) The clustering sizes of nano-ZrO<sub>2</sub> and nano-SiO<sub>2</sub> particles after four FSP passes are usually around 150 ~ 200 nm and 200 ~ 300 nm, respectively. The average grain size of the AZ31 matrix of the 4P FSP composites could be effectively refined to 2 ~ 4  $\mu\text{m}$ , as compared with the  $\sim 6\ \mu\text{m}$  in the FSPed AZ31 alloy (without particles) processed under the same FSP condition. The crystalline ZrO<sub>2</sub> phase is very stable, no reaction between ZrO<sub>2</sub> and Mg occurred during the FSP mixing ZrO<sub>2</sub> into Mg-AZ31 matrix.
- (3) The hardness and tensile properties at room temperature of the AZ31 composites with nano-fillers were appreciably improved, as compared with the AZ31 cast billet.

## Acknowledgements

The authors would like to gratefully acknowledge the sponsorship from National Science Council of Taiwan, ROC, under the projects NSC 93-2216-E-110-021 and 94-2216-E-110-010.

## References

- [1] B.Q. Han and D.C. Dunand: Mater. Sci. Eng. A Vol. 277 (2000), p. 297.
- [2] D.M. Lee, S.K. Suh, B.G. Kim and J.S. Lee: Mater. Sci. Tech. Vol. 13 (1997), p. 590.
- [3] L.Hu and E. Wang: Mater. Sci. Eng. A Vol. 278 (2000), p. 267.
- [4] R.A. Saravanan and M.K. Surappa: Mater. Sci. Eng. A Vol. 276 (2000), p. 108.
- [5] C.Y. Chen and Chi Y. A. Tsao: Mater. Sci. Eng. A Vol. 383 (2004), p. 21.
- [6] W.M. Thomas, E.D. Nicholas, J.C. Needham, M.G. Church, P. Templesmith, and C.J. Dawes, International patent no. PCT/GB92/02203 and GB Patent no. 9125978.8 1991.
- [7] R.S. Mishra, M.W. Mahoney, S.X. McFadden, N.A. Mara and A.K. Mukherjee: Scripta Mater. Vol. 42 (2000), p. 163.
- [8] Z.Y. Ma, R.S. Mishra and M.W. Mahoney: Acta Mater. Vol. 50 (2002), p. 4419.
- [9] P.B. Berbon, W.H. Bingel, R.S. Mishra, C.C. Bampton and M.W. Mahoney: Scripta Mater. Vol. 44 (2001), p. 61.
- [10] D.T. Zhang, M. Suzuki and K. Maryama: Scripta Mater. Vol. 52 (2005), p. 899.
- [11] C.I. Chang, C.J. Lee and J.C. Huang: Scripta Mater. Vol. 51 (2004), p. 509.
- [12] R.S. Mishra, Z.Y. Ma and I. Charit: Mater. Sci. Eng. A Vol. 341 (2003), p. 307.
- [13] C.J. Lee, J.C. Huang and P.J. Hsieh: Scripta Mater. Vol. 54 (2006), p. 1415.

- 
- [14] H.K. Lin and J.C. Huang: Mater. Trans. JIM Vol. 43 (2002), p. 2424.
  - [15] Y.N. Wang, C.J. Lee, H.K. Lin, C.C. Huang and J.C. Huang: Mater. Sci. Forum Vol. 426-432 (2003), p. 2655.
  - [16] Y.N. Wang, C.I. Chang, C.J. Lee, H.K. Lin and J. C. Huang: Scripta Mater. Vol. 55 (2006), p. 637.